Surface Science 606 (2012) 34–39

Contents lists available at SciVerse ScienceDirect

Surface Science

journal homepage: www.elsevier.com/ locate/susc

Adsorption and desorption characteristics of 3-dimensional networks of fused graphene

Mohammad Choucair [a,*], Nicholas M.K. Tse [a], Matthew R. Hill [b], John A. Stride [a,c]

[a] School of Chemistry, University of New South Wales, Sydney 2052, Australia
[b] CSIRO Division of Materials Science and Engineering, Private Bag 33, Clayton South MDC, Victoria 3169, Australia
[c] Bragg Institute, Australian Nuclear Science and Technology Organisation, PMB 1, Menai, NSW 2234, Australia

ARTICLE INFO

Article history:
Received 7 July 2011
Accepted 22 August 2011
Available online 28 August 2011

Keywords:
Graphene
Nitrogen adsorption
Methylene blue
Defects

ABSTRACT

Here we explore the exceptional structural characteristics of a set of graphene-related materials prepared by a wet chemical approach. We present a comprehensive study of the effects of morphology, sonication, temperature, probe species, and stacking behaviour on the measurement of graphene surface area. Nitrogen gas was used in the solid state gas adsorption measurements and methylene blue dye for adsorption measurements on aqueous dispersions of graphene. The surface area values obtained are among the highest reported for synthetic graphenes: 1700 $m^2 g^{-1}$ in aqueous dispersions and 612 $m^2 g^{-1}$ in the solid state. Microscopy revealed the graphene used in the study was present in large part as free sheets and electron diffraction confirmed the successful synthesis of high quality graphene with a regular C–C bond length of 1.41 ± 0.02 Å.

1. Introduction

Since the isolation of free graphene sheets reported in 2004 by Novoselov et al. [1], it has developed into a major focus of study in the science of carbon-based materials, due in part to its exceptional properties at the atomic scale and the very nature of this most fundamental of materials [1–3]. Until recently, the piece-meal synthesis of graphene has limited the study of the bulk physical properties, however various remarkable properties have been attributed to it in some truly exceptional experiments performed on isolated sheets [3–6].

Graphene is a material which is essentially all surface. If both sides of a graphene sheet are considered, then the effective surface area is extremely large, 2630 $m^2 g^{-1}$. This has led many researchers to consider it as a potential candidate material in applications benefiting from extreme surface areas [7,8]. However, the functionality and performance of emerging graphene-based technologies will be heavily dependent on the ability to control the extent of surface availability [9–11]. Different synthesis methods yielding bulk quantities of graphene ultimately converge on the same issue: identifying the *most appropriate* post-synthesis fabrication method while retaining a set of favoured physical properties necessary for an envisioned technology.

To date, bulk physical properties have been investigated on graphene-related materials [12], chemically modified graphene [13], graphene oxide paper [14], and composites incorporating graphene [15]. The reported Brunauer–Emmett–Teller (BET) surface areas for graphene by nitrogen gas adsorption have indicated that values are much lower than the theoretical maximum largely due to the agglomeration of individual graphene sheets [12,13]. Our recent development of a chemical synthesis pathway to gram-scale quantities of graphene [16] has allowed for the thorough elucidation of the various parameters that affect the measurement of surface areas of porous fused graphene structures and free sheets, in the solid state and as aqueous dispersions, respectively.

2. Materials and methods

All of the graphene samples studied herein were obtained by the solvothermal reaction of sodium and ethanol [16]. Reactions were performed in either a 25 ml Teflon-lined Parr Instrument Company 4749 reactor or 125 ml Titanium Parr Instrument Company 4750 reactor. Typical synthesis consists of heating a 1:1 molar ratio of sodium (ca. 2 g) and alcohol precursor (*e.g.* 5 ml of ethanol) in a sealed reaction vessel at 220 °C for 72 h to yield the solvothermal product. This material is then rapidly pyrolysed in air and the resulting material purified in 1 g batches. Acid washed decolourising charcoal (BDH Chemicals), and 98–99% natural graphite (Hopkins and Williams) were used for comparative purposes. Impurity levels in all samples were obtained by X-ray photoelectron spectroscopy (XPS), unless otherwise stated. Characterisation measurements are described in the Supporting Information.

2.1. Sample preparation

For the summary of sample preparation, see Table 1.

* Corresponding author. Tel./fax: +61 2 93854672.
E-mail address: m.choucair@unsw.edu.au (M. Choucair).

0039-6028/$ – see front matter © 2011 Elsevier B.V. All rights reserved.
doi:10.1016/j.susc.2011.08.016

Table 1
Summary of sample preparation methods.

Sample	Precursor	Purification method
1	Ethanol	Stirring in 100 ml of milliQ water for 96 h, then washed by vigorous shaking in 300 ml of milliQ water 5 times with vacuum filtration between each wash. The product was collected and dried under vacuum for 24 h at 130 °C and contains less than 7 wt.% impurities.
1b	Ethanol	Sample **1** purified further by stirring in 100 ml of slightly acidified ethanol for 24 h. The product was washed with an ethanol–water mixture upon filtration, collected and dried under vacuum for 1 h at 130 °C. The final sample contains less than 1 wt. % impurities.
2	Ethanol	Stirring in 100 ml of milliQ water for 1 h, vacuum filtered, and stirred in 100 ml of slightly acidified ethanol for 1 h. The product was washed with an ethanol-water mixture upon filtration, collected and dried under vacuum for 1 h at 130 °C.
3	Ethanol	Stirring in 100 ml of milliQ water for 24 h, vacuum filtered, and stirred in 25 ml of slightly acidified ethanol for 24 h. The product was washed with an ethanol–water mixture upon filtration, collected and dried under vacuum for 24 h at 130 °C; the final sample contains less than 1 wt.% impurities.
4	Ethanol	Sample **2** sonicated for 6 h in ethanol, collected by rotary evaporation of ethanol, and drying under vacuum for 24 h at 130 °C.
5	Methanol	Stirring in 100 ml of milliQ water for 1 h, vacuum filtered, and stirred in 100 ml of slightly acidified ethanol for 1 h. The product was washed with an ethanol–water mixture upon filtration, collected and dried under vacuum for 1 h at 130 °C.

3. Results and discussion

Contrary to initial expectations, the lowest BET surface area was obtained from the sample believed to have the greatest quantity of free sheets, sample **1**, Table 2. The pore size distribution for this sample, (Figure S1 and Table S1, Supporting Information), indicates most pores are in the 1–10 μm range, with a median pore size of 4.50 μm, whilst the sample displayed a porosity of 91%. The difference between the total pore volume (BET, 0.039 $cm^3\,g^{-1}$) and the total intrusion volume (Hg, 4.69 $cm^3\,g^{-1}$) is due to the fact that the mercury adsorption technique takes into account much larger pore sizes, including voids due to inter-particle packing, in contrast to the BET method. This result indicates that the sample is non-uniform, with a range of length scales.

The apparent density of sample **1** as determined by mercury porosimetry (2.18 g cm^{-3}) (Table S1, Supporting Information) lies well within the commonly observed values for graphite (2.09–2.23 g cm^{-3}),[1] whilst the relatively low BET surface area of 11.3 $m^2\,g^{-1}$ confirms the absence of significant mesoporosity (2–50 nm), suggesting that the graphene is present as large discrete sheets, in accord with the Hg intrusion data (Fig. 1).

The BET data for the sample that underwent only mild agitation, **3**, showed more than an order of magnitude increase (153 $m^2\,g^{-1}$) over sample **1**. It is therefore essential to consider washing time when measuring surface area. Furthermore, increased specific surface areas were generally observed for samples having higher porosity, with the methanol-sourced sample, **5**, displaying the largest BET surface area at 484 $m^2\,g^{-1}$, comparable to the maximum surface area obtained for an ethanol based graphene, **2,** of 477 $m^2\,g^{-1}$.

The large hysteresis observed in the gas desorption branches suggests the adsorbed gas molecules are partially trapped within the highly porous materials, Fig. 2. Notably, the trapping effect was not observed for samples exhibiting low BET surface areas (samples **1** and **4**). The trapping results from the sample pores being of similar size to the kinetic diameter of the probe gas, nitrogen. Given this size constraint, adsorption is most likely limited to monolayers. Thus the Langmuir equation is more appropriate when calculating surface areas of highly porous materials as it assumes monolayer adsorption rather than the multilayer process taken into account by the BET equation [17]. In this regard, Langmuir surface areas for samples **2** and **5** were calculated to be 598 $m^2\,g^{-1}$ and 612 $m^2\,g^{-1}$ respectively.

Table 2
Summary of the gas adsorption results and pore data obtained.

Solid state surface area analysis of the different graphene samples					
	Sample 1	Sample 2	Sample 3	Sample 4	Sample 5
SA_{BET} ($m^2\,g^{-1}$)	11.3	477	153	21.7	484
Total pore volume ($cm^3\,g^{-1}$)[a]	0.039	0.32	0.17	0.075	0.62
Micropore volume ($cm^3\,g^{-1}$)[b]	0.00052	0.17	0.048	0.0056	0.15
Micropore surface area ($m^2\,g^{-1}$)[b]	0.1	397	100	11.9	325
$SA_{Langmuir}$ ($m^2\,g^{-1}$)	15.3	598	195	29.9	612

[a] Calculated at $P/P_o = 0.99$.
[b] Calculated using t-plot analysis.

As the samples contained low levels of impurities of up to 7 wt.% (NaOH, Na_2O, TiO_2, see Table S2 Supporting Information), the effect of particle coverage on the measurement of surface area was considered. However, the contributions by impurities that affected the solid state measurements were found to be far less than that of porosity. This can be most easily seen with samples **2** and **5.** Both have similar pre-treatments and no impurities with similar elemental composition and correspondingly similar BET surface areas, Table 2. Although, when a large number of impurities were present on the surface, ca. 20wt.%, they were found to block adsorption sites that then prohibit maximal gas loading. Removal of these impurities allowed the full carbon surface area to be exposed, resulting in an adsorption surface area more in accord with the true absolute area (Figure S3, Supporting Information).

The same samples analyzed by gas adsorption were also investigated by MB in order to compare the surface areas obtained between the two techniques. Surface areas observed by N_2 adsorption were consistently lower than those recorded in solution experiments with MB, Fig. 3. This indicated that a smaller fraction of the sample surface was accessible under low partial pressures of N_2 at 77 K,

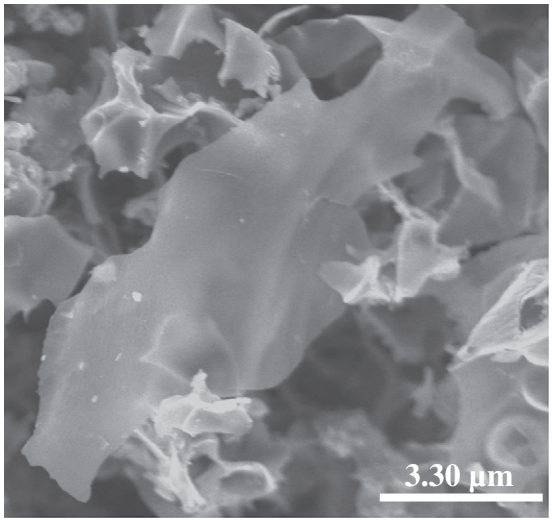

Fig. 1. Scanning electron microscope image (SEM) of a large sheet of graphene in sample **1**. The graphene sheet is almost fully transparent under the beam. Further SEM images can be found in Supporting Information Figures S2 and S3.

[1] Graphite Mineral Data, viewed 16 December 2009, (http://webmineral.com/data/Graphite.shtml).

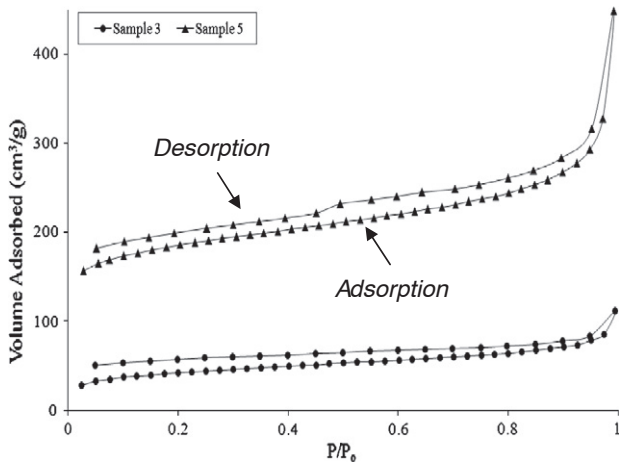

Fig. 2. Typical nitrogen adsorption–desorption isotherms for synthesized graphene samples at 77 K.

when compared to ambient conditions in solution. A corollary to this is that there must also be many surfaces that are effectively not exposed to gas adsorption, *i.e.* the space between graphene layers approaches the kinetic diameter of the gas probe species.

MB adsorption has been widely used as a measure of the surface areas of graphitic materials. The accepted calibration being that each milligram of adsorbed MB represents 2.45 m^2 of specific surface area [18]. The values for samples sonicated for 1 h are summarized below together with the gas adsorption values, Fig. 3. The MB surface area values for natural graphite (9.70 $m^2\,g^{-1}$) and charcoal (521.14 $m^2\,g^{-1}$) tend to agree with literature values reported by both the MB technique and gas adsorption (ca. 7–15 $m^2\,g^{-1}$ for graphite, and ca. 300–1000 $m^2\,g^{-1}$ for charcoal), with the range in reported values largely due to sample pre-treatment [19–23]. The values obtained for the graphene samples were much greater than the other carbons investigated and the MB analysis of the samples tend to complement the BET and Langmuir surface areas. Whilst the MB results for samples **2** and **5** (810 and 936 $m^2\,g^{-1}$) are similar and in accord with the BET and Langmuir data, those samples having undergone greater mechanical perturbation prior to analysis (samples **1b** and **3**), showed much larger surface areas (1462 $m^2\,g^{-1}$ and 1240 $m^2\,g^{-1}$ respectively).

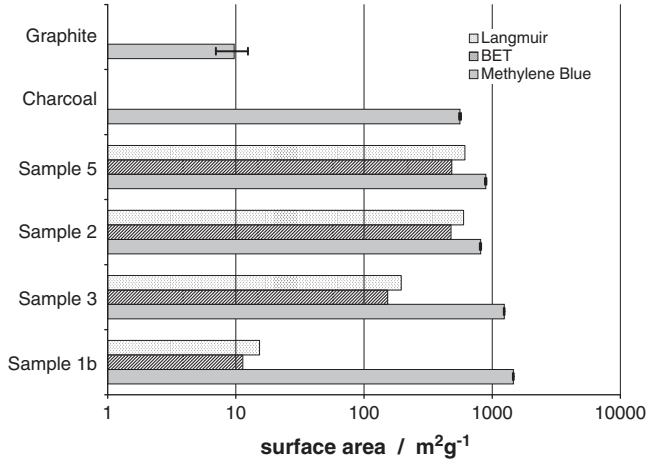

Fig. 3. Comparison of the surface areas obtained by gas (from BET and Langmuir isotherms) and 1 h sonication MB adsorptions for different graphene samples. Also shown are the MB values for charcoal and graphite. The uncertainty values upon reproducibility for the MB results were typically less than 2% of the reported surface areas at a 95% level of confidence with the exception of the graphite sample ($U = 27.94\%$), and were calculated according to Hibbert [24].

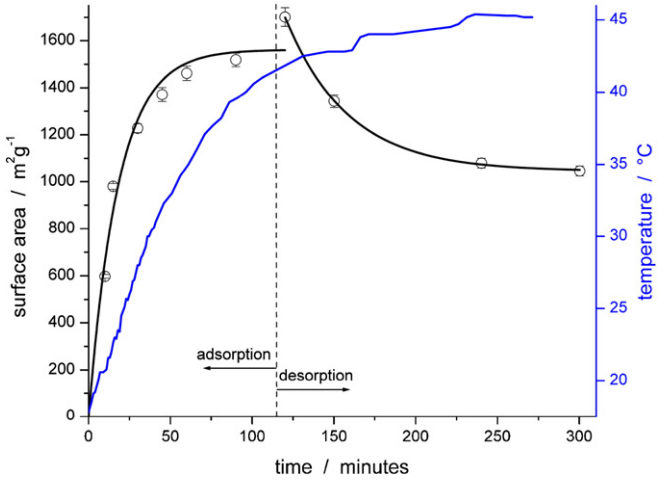

Fig. 4. Plot of surface area obtained by the MB technique as a function of sonication time for sample **1b**, with the increase in temperature of the sonication bath overlaid to highlight the effect of temperature. The uncertainty values for the surface area values obtained for sample **1b** were typically less than 1% of the reported surface areas at a 95% level of confidence, and were calculated according to Hibbert [24].

The degree of mechanical perturbation of the samples prior to MB adsorption determines the extent of free sheets, existing as fragmentation products of the 3-D porous network. The diffusion kinetics favour the adsorption of MB onto free sheets over the porous structure as the dye molecules need not permeate through open pores. A greater quantity of free graphene sheets therefore corresponds to a greater surface area, meaning that the surface area should increase with sonication time, Fig. 4 (Supp. Info S4).

The sample containing the greatest number of free sheets corresponds to the highest MB surface area, **1b** (1700 $m^2\,g^{-1}$), a trend continued with samples of decreasing surface area and increased porosity, Fig. 3. The plots showing the effect of sonication time on surface area for samples **1b** and **3** (Figure S4 Supp. Info.) show a maximum surface area at similar periods of sonication, before decreasing slightly with additional sonication. This apparent decrease in surface area is explained by the temperature of the water in the sonication bath over the sonication period of 6 h, reaching ca. 319 K after 2 h of sonication. This increase of more than 20 K over the initial temperature is simply a result of the heating effects of

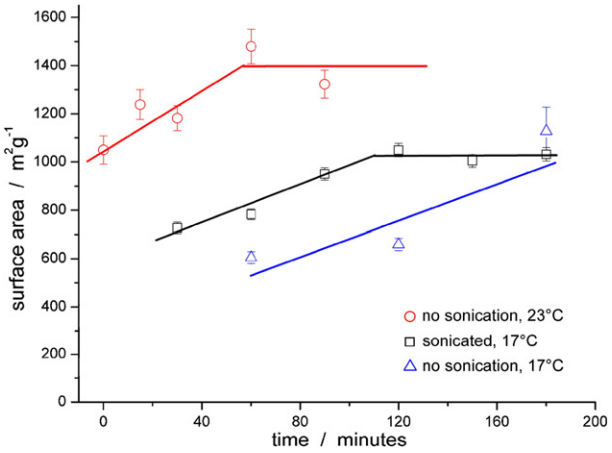

Fig. 5. Plot showing the surface area values obtained for non-sonicated sample **1b** at constant temperatures of 17 °C (290 K), 23 °C (296 K), and sonicated samples of **1b** at a constant temperature of 17 °C (290 K). The uncertainty values for the MB results were typically less than 5% of the reported surface areas at a 95% level of confidence, with the exception of the surface area of 180 min non-sonicated sample at 17 °C, ($U = 5.76\%$), and were calculated according to Hibbert [24].

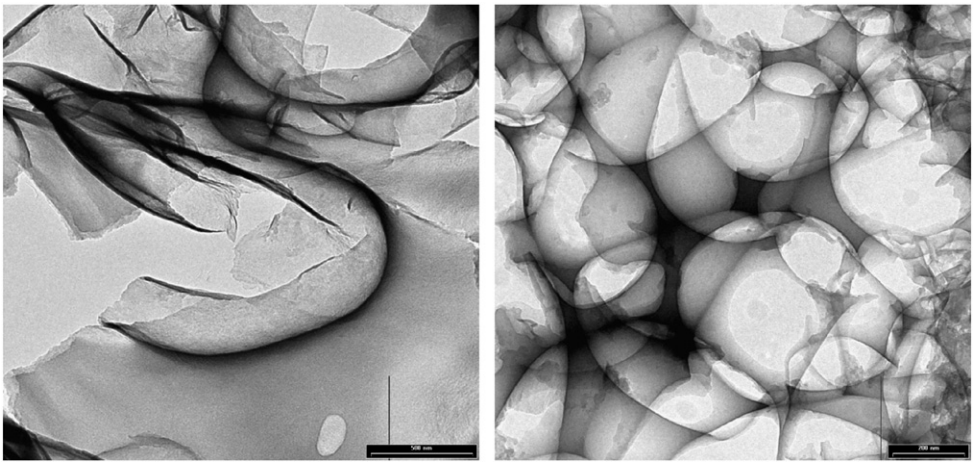

Fig. 6. Typical TEM images of (*left*) ethanol derived and (*right*) methanol derived samples. Scale bars (*left*) 500 nm and (*right*) 200 nm. Regions of relative opacity indicate folds or overlap within the sheets. The ethanol samples appear as large sheets with crimping and layering evident whereas the methanol samples show a more rigid structure.

sonication, Fig. 4. These non-isothermal conditions mean that the equilibrium dynamics of MB adsorption and desorption naturally result in a maximum in the measured surface area.

In order to further investigate the effects of sonication and temperature on the measured values, experiments were conducted on sample **1b**, under isothermal conditions at 290 K and 296 K without sonication and at 290 K with sonication, Fig. 5. The optimisation of temperature was found to be essential, as a significant difference in the surface area was obtained with just a 6 K change in temperature. An average surface area of 1305 $m^2 g^{-1}$ was measured at 296 K during the first 2 h. which was more than double the average surface area obtained at 290 K over the same period, 632 $m^2 g^{-1}$. After 30 min. of sonication and at 290 K the sample required 50% more sonication to approach the surface area observed at 296 K, ca. 1182 $m^2 g^{-1}$.

Whilst increased molecular mobility may lead to increased adsorption, at some temperature the increased mobility acts to desorb MB molecules. This is due to an increase in collisions and the Boltzmann factor, which favours increased desorption. When the sample was maintained at a constant temperature of 290 K the surface areas

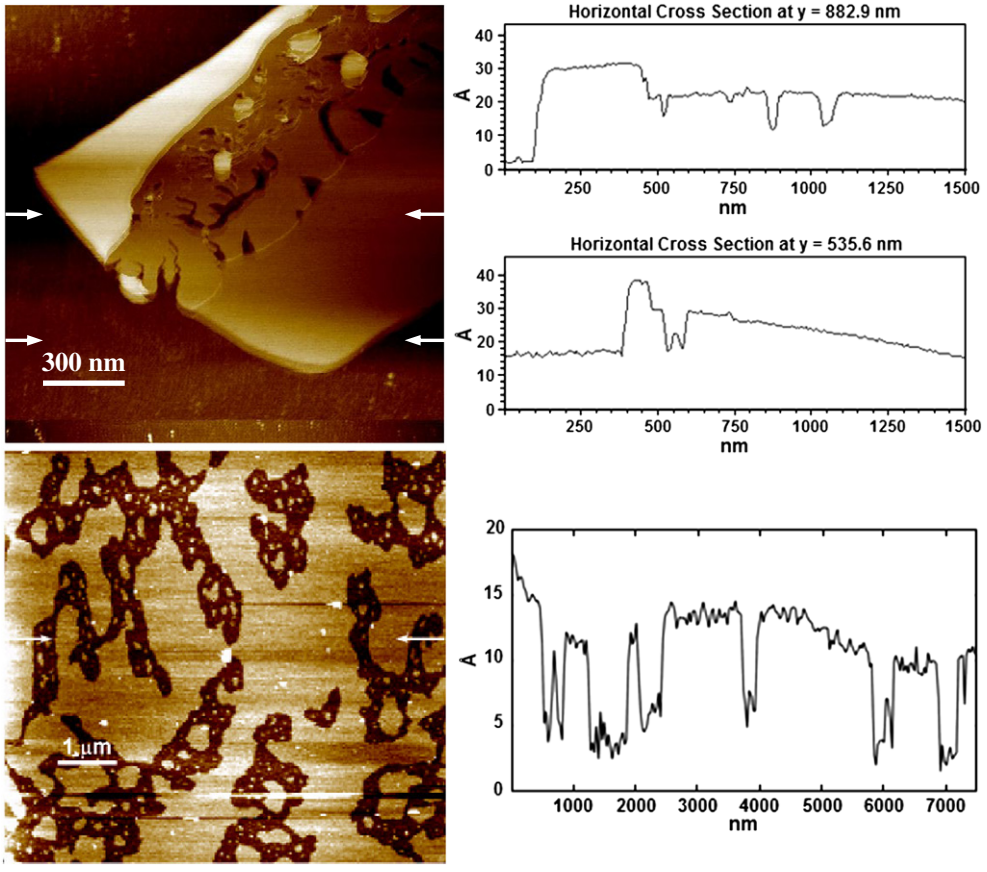

Fig. 7. AFM images (*top*) of a methanol derived sample, **5**, and (*bottom*) an ethanol derived sample, **1b**. Both show the tendency for the sheets to form layers.

with and without sonication clearly display the effects of physical agitation. The kinetics of the MB solution and the effects on the interaction of the dye with the graphene play a major role in the determination of the surface area by this method.

Agglomeration of graphene sheets is commonly referred to in literature to explain the apparent decrease in measured surface area of bulk graphene from the theoretical value [12]. Layering, crimpling, and folding is indeed observed in our samples under TEM, Fig. 6. In addition, the porosity of the samples is believed to affect the measured MB surface area. For example, the measured MB surface area of the methanol-derived sample **5** was constant around ca. 951 $m^2 g^{-1}$ rather than displaying a peak value (Figure S4, Supporting Information). This is believed to be due to sample **5** not readily breaking up under sonication as the high number of small pores act to increase the rigidity of the structure, rendering it less prone to fragmentation. This is supported by the gas adsorption data, Table 2.

AFM topographies of samples **5** and **1b** showed porous sheets with a tendency to layer one on top of another, Fig. 7. The ethanol derived sample showed step heights of 5 Å and 10 Å indicating fragments of single and bi-layered sheets. The methanol derived sample showed much greater abilities to layer with a larger fragment of greater than 25 Å in thickness having layers of ca. 5 Å. Single area electron diffraction (SAED) patterns also showed the sheets form few layers (Fig. 8). This layering is believed to be related to offset overlapped π–π interactions caused by defects (Figure S5, Supporting Information). The more defective the graphene, the greater the offset. Hence, the reduced ability of the sheets to tend towards a 3-dimensional graphitic structure, *i.e.* having a higher degree of dispersion. This in turn affects the measurable MB surface area.

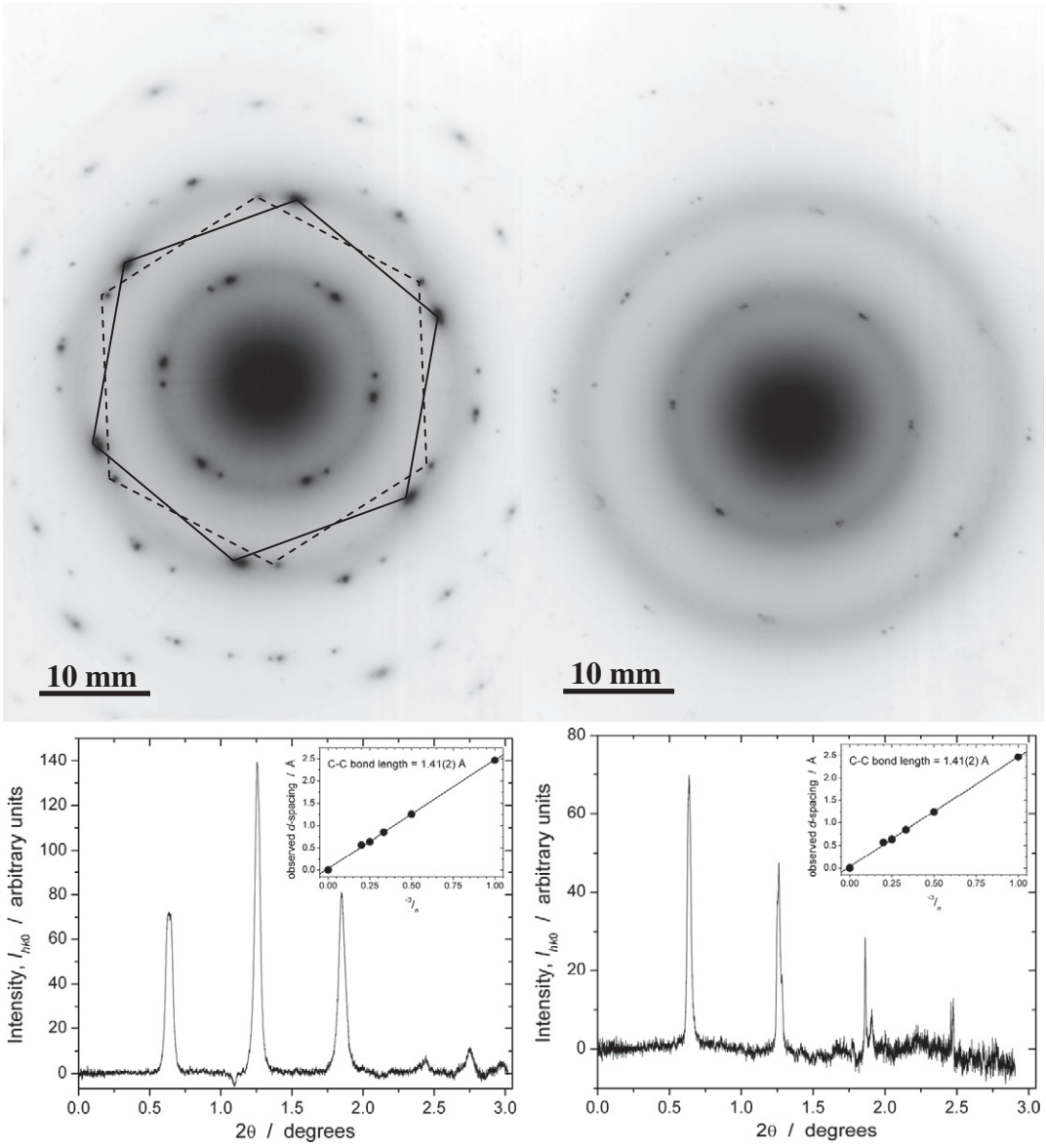

Fig. 8. Single area electron diffraction (SAED) patterns of (*left*) an ethanol derived sample (focal length 900 mm, 10° offset), and (*right*) a methanol derived sample (focal length 1010 mm, 2° offset). The spots are indicative of free graphene sheets, having a regular C–C bond length of 1.41 ± 0.02 Å layered on top of one another, with small angular offsets. The off-set is determined from the angle between the two sets of spots. This is obtained by drawing hexagons connecting the points in each pattern (*left*), and calculating the angle one hexagon would need to be rotated by to get to the other—with the maximum being 60° as this translates one point on the hexagon to an equivalent point. Lower plots are background-corrected plots of the respective samples, integrated along the (*hk*0) directions, having *d*-spacings of $\sqrt{3}/n$.

4. Conclusions

An integrated set of characterisation techniques have been utilized to probe the structure of a novel series of graphene related materials. It was shown that the experimental conditions required by the characterisation technique including temperature, sample morphology, washing time, and sonication strongly affected the surface accessible to the probe species. Nitrogen adsorption was affected by the consolidation of the graphene layers at 77 K, whereas kinetic effects influenced the outcome of MB adsorption. Nevertheless, the surface area values obtained from these samples were among the highest reported for synthetic graphenes (MB 1700 $m^2 g^{-1}$, N_2 612 $m^2 g^{-1}$), all the more remarkable given the facile synthetic procedure.

Acknowledgements

This research was supported by an Australian Postgraduate Award to M.C. Microscopy facilities courtesy of the electron microscope units at the University of New South Wales and the University of Sydney. M.R.H acknowledges funding from the CSIRO Hierarchical Materials Emerging Science Initiative.

Appendix A. Supplementary data

Supplementary data to this article can be found online at doi:10.1016/j.susc.2011.08.016.

References

[1] K.S. Novoselov, A.K. Geim, S.V. Morozov, D. Jiang, Y. Zhang, S.V. Dubonos, et al., Science 306 (2004) 666.
[2] Y. Zhang, Y.W. Tan, H.L. Stormer, P. Kim, Nature 438 (2005) 201.
[3] A.K. Geim, K.S. Novoselov, Nat. Mater. 6 (2007) 183.
[4] X. Li, X. Wang, L. Zhang, S. Lee, H. Dai, Science 319 (2008) 1229.
[5] Y. Hernandez, V. Nicolosi, M. Lotya, F.M. Blighe, Z. Sun, S. De, et al., Nat. Nanotechnol. 3 (2008) 563.
[6] V.C. Tung, M.J. Allen, Y. Yang, R.B. Kaner, Nat. Nanotechnol. 4 (2008) 25.
[7] L. Schlapbach, A. Züttel, Nature 414 (2006) 353.
[8] S. Patchkovskii, J.S. Tse, S.N. Yurchenko, L. Zhechkov, T. Heine, G. Seifert, Proc. Natl. Acad. Sci. U. S. A. 102 (30) (2005) 10439.
[9] S.-L. Chou, J.-Z. Wang, M. Choucair, H.-K. Liu, J.A. Stride, S.-X. Dou, Electrochem. Commun. 12 (2) (2010) 303.
[10] H. Wang, Y. Yang, Y. Liang, J.T. Robinson, Y. Li, A. Jackson, et al., Nano Lett. 11 (2011) 2644–2647.
[11] Z.-S. Wu, W. Ren, L. Xu, F. Li, H.-M. Cheng, ACS Nano 5 (2011) 5463–5471.
[12] S. Stankovich, D.A. Dikin, R. Piner, K.A. Kolhaas, A. Kleinhammes, Y. Jia, et al., Carbon 45 (2007) 1558.
[13] H.C. Schniepp, J.L. Li, M.J. McAllister, H. Sai, M. Herrera-Alonso, D.H. Adamson, et al., J. Phys. Chem. B 110 (2006) 8535.
[14] D.A. Dikin, S. Stankovich, E.J. Zimney, R.D. Piner, G.H.B. Dommett, G. Evmenenko, et al., Nature 448 (2007) 457.
[15] S. Stankovich, D.A. Dikin, G.H.B. Dommett, K.M. Kohlhaas, E.J. Zimney, E.A. Stach, et al., Nature 442 (2006) 282.
[16] M. Choucair, P. Thordarson, J.A. Stride, Nat. Nanotechnol. 4 (2009) 30.
[17] S.J. Gregg, K.S.W. Sing, Adsorption, Surface Area and Porosity, Academic Press London, London, 1982.
[18] H.P. Boehm, A. Clauss, G.O. Fischer, U. Hofmann, Anorg. Allg. Chem. 316 (1962) 119.
[19] C. Hontoria-Lucas, A.J. Lopez-Peinado, JdD Lopez-Gonzalez, M.L. Rojas-Cervantes, R.M. Martin-Aranda, Carbon 43 (1995) 1585.
[20] K.S.W. Sing, D.H. Everett, R.A.W. Haul, L. Moscou, R.A. Pierotti, J. Rouquerol, et al., Pure Appl. Chem. 57 (4) (1985) 603.
[21] S. Wang, Z.H. Zhua, A. Coomes, F. Haghseresht, G.Q. Luc, J. Colloid Interface Sci. 284 (2005) 440.
[22] F. Marken, M.L. Gerrarda, I.M. Mellora, R.J. Mortimera, C.E. Maddena, S. Fletcera, et al., Electrochem. Commun. 3 (2001) 177.
[23] H. Hermanna, T. Schubertb, W. Grunera, N. Matterna, Nanostruct. Mater. 8 (1997) 215.
[24] D.B. Hibbert, Analyst 131 (2006) 1273.